BNL-221945-2021-JAAM

Hydroxymethanesulfonate (HMS) Formation during Summertime Fog in an Arctic Oil Field

J. Liu, T. B. Watson

To be published in "Environmental Science and Technology Letters"

July 2021

Environmental and Climate Sciences Department

Brookhaven National Laboratory

U.S. Department of Energy

USDOE Office of Science (SC), Biological and Environmental Research (BER) (SC-23)

DISCLAIMER

Hydroxymethanesulfonate (HMS) Formation during Summertime Fog in an Arctic Oil Field

Jun Liu, Matthew J. Gunsch, Claire E. Moffett, Lu Xu, Rime El Asmar, Qi Zhang, Thomas B. Watson, Hannah M. Allen, John D. Crounse, Jason St. Clair, Michelle Kim, Paul O. Wennberg, Rodney J. Weber, Rebecca J. Sheesley, and Kerri A. Pratt*

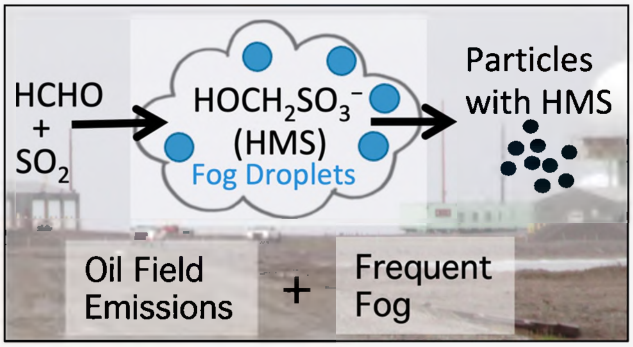

ABSTRACT: Hydroxymethanesulfonate (HMS) is produced in the aqueous-phase reaction of formaldehyde (HCHO) and sulfur dioxide (SO_2) and has been proposed as a significant contributor to midlatitude wintertime pollution events. Here we report HMS detection within submicrometer atmospheric aerosols during frequent late summer, regional fog events in an Arctic oil field. The number fraction of individual particles containing HMS increased during fog periods, consistent with aqueous-phase formation. The single-particle mass spectra showed the primary particle signature (oil field emissions), plus secondary oxidized organics and sulfate, consistent with aqueous-phase processing. HMS mass concentrations ranged from below the ion chromatography limit of detection (0.3 ng/m^3) to 1.6 ng/m^3, with sulfate concentrations of 37−222 ng/m^3. HCHO and SO_2 measurements suggest that the fog HMS production rate is ~10 times higher in the oil fields than in the upwind Beaufort Sea. Aqueous-phase reactions of local oil field emissions during frequent summertime regional fog events likely have downwind impacts on Arctic aerosol composition. The potential for fog-based HMS production was estimated to be an order of magnitude higher in Fairbanks and Anchorage, AK, than in the oil fields and may explain the missing organosulfate source contributing to Fairbanks air quality.

INTRODUCTION

Aqueous-phase reactions in fog and cloud droplets often yield products that persist after droplet evaporation and contribute to aerosol production.[1−5] The majority of global atmospheric sulfate (80−90%) is estimated to be formed through aqueous-phase hydrogen peroxide and ozone oxidation of sulfur(IV) to sulfur(VI).[6−8] Munger et al.[9] measured S(IV) and formaldehyde (HCHO) concentrations in fog and cloud droplets in California that exceeded their expected saturation concentrations from Henry's law calculations.[9,10] The excess S(IV) corresponded to hydroxymethanesulfonate (HMS, $HOCH_2SO_3^-$) formed from the aqueous reaction between HCHO and sulfur dioxide (SO_2).[9,10] Globally, HCHO is produced by hydrocarbon oxidation,[11] fossil fuel combustion,[12] and biomass burning.[13] Major sources of SO_2 include fossil fuel combustion and industry,[14,15] as well as the ocean and volcanoes.[16,17] A theoretical investigation proposed that an HMS isomer, hydroxymethyl sulfite, can also be produced through the aqueous-phase reaction between SO_2 and HCHO.[18]

HMS has been measured in fogwater,[9,19−23] precipitation,[24−26] and aerosol particles.[27−35] HMS production is favored within fog and cloud droplets, compared to aerosol, in part due to the increased pH. In particular, single-particle mass spectrometry provides HMS identification within individual atmospheric particles by detection of its molecular ion [m/z −111 ($HOCH_2SO_3^-$)].[36−38] Whiteaker et al.[36] first observed individual particles containing HMS during fog events in Bakersfield, CA. HMS-enriched single particles have since been observed during fog in London, England,[39] and Guangzhou, China,[40] as well as winter haze in Beijing, China.[32,33] In summertime Atlanta, GA, 10−15% of measured individual particles contained HMS, which often coexisted in the same particles as carboxylic acids and other oxidized organic compounds indicative of aqueous processing.[41,42] Recent studies[32−35,43] proposed that the HMS concentration can reach significant levels in China during winter haze and may be misidentified as sulfate. HMS formation may explain high particulate sulfur concentrations in Beijing,[43] with wintertime concentrations of up to 7.3 $\mu g/m^3$.[3,35] Song et al.[32] showed that Beijing sulfate model predictions improve through the inclusion of HMS formation. Moch et al.[34] and Song et al.[44] recently presented observational and modeling evidence of the global presence of HMS.

In the Arctic, there is growing attention on the significance of local combustion emissions, including from large oil fields across the region.[45−47] However, few measurements of atmospheric trace gases and aerosols within Arctic oil fields exist,[48−52] with none, to the best of our knowledge, examining subsequent aqueous-phase processing. The formation, dissipation, and droplet size distribution of Arctic fog, as well as aerosol interactions, have previously been investigated,[53−55] with fog frequently observed on the North Slope of Alaska during summertime.[56,57] As the third largest oil field in North America, the North Slope of Alaska oil fields cover ~14000 km^2. In this study, local combustion emissions[46,48,50,51] and fog processing were investigated using an aerosol time-of-flight mass spectrometer (ATOFMS)[58] during August and September 2016 at Oliktok Point, AK, within the oil fields. The ATOFMS measured the size and chemical composition of individual particles, a fraction of which contained HMS, which was quantified using ion chromatography (IC). Constrained by aircraft near-surface measurements of SO_2 and HCHO, HMS production rates were estimated for the oil fields and compared to those of the upwind Beaufort Sea and two cities in Alaska.

■ MATERIALS AND METHODS

Atmospheric measurements were conducted at the Atmospheric Radiation Measurement (ARM) Mobile Facility (AMF3) located at Oliktok Point, AK (70°29′41.4″ N, 149°53′10.9″ W). Meteorological data, including temperature, wind speed, wind direction, relative humidity (RH), and precipitation, were obtained from a Vaisala WXT520 weather transmitter at a height of ~10 m. Ambient visibility was obtained by a visibility sensor (Vaisala PWD). Weather data from the three closest airports were also used to identify fog events. These were the airports at Deadhorse (70°11′24″ N, 148°27′36″ W), Ugnu-Kupruk (70°19′52″ N, 149°35′39″ W), and Nuiqsut (70°12′32″ N, 151°0′20″ W), which are located 20−70 km from Oliktok Point (Figure S1). Meteorological data were also included from Utqiaġvik (71°17′41″ N, 156°45′52″ W, formerly known as Barrow), which is the largest city of the North Slope Borough and is 270 km northwest of Oliktok Point.

ATOFMS[58] measurements were conducted from August 22 to September 17, 2016, using a PM_{10} (<10 μm particulate matter) cyclone inlet (URG Corp., Chapel Hill, NC) and are described by Gunsch et al.[49] The ATOFMS measured 32880 individual particles from 0.07 to 1.6 μm (vacuum aerodynamic diameter). As summarized by Gunsch et al.[49] and in the Supporting Information, ART-2a clustering analysis[59] identified eight single-particle types, with number concentration percentages shown in parentheses: organic carbon (OC)-amine-sulfate (45%), sea spray aerosol (15%), OC (16%), elemental carbon (EC, 2%), EC and OC (ECOC, 10%), biomass burning (8%), mineral dust (3%), and incineration particles (1%). HMS-containing particles were identified by searching the individual particle mass spectra for m/z −111 ($HOCH_2SO_3^-$), based on previous field and laboratory work,[36] using a threshold of 0.01 relative peak area. The isomer hydroxymethyl sulfite, recently predicted from theoretical work,[18] cannot be distinguished using this method. HMS could not be identified in sea spray aerosol, because of the lack of m/z −111 formation by $NaCH_3SO_4$,[37,38] in incineration particles, because of the KCl_2^- isobaric interference, or in OC and biomass burning particles, because of the lack of negative ion mass spectra due to water accumulation during transport.[37]

From August 18 to September 18, 2016, 10 PM_1 (<1 μm particulate matter) samples were collected on 90 mm diameter quartz fiber filters over 1−4 day periods using a medium volume sampler (URG Corp.). HMS and sulfate were separated and quantified (Figure S2) using a Metrohm Peak Ion Chromatograph (Compact 761, Metrohm, Herisau, Switzerland), operated with a 250 μL sample loop and a Metrosep A Supp 5-150/4.0 anion column with 3.2 mM $Na_2(CO_3)$/1.0 mM $NaHCO_3$ eluent. Uncertainty in measured HMS mass concentrations is estimated to be 20% + the limit of detection, which ranged from 0.3 to 1 ng/m^3. Additional sampling and IC details are provided in the Supporting Information.

SO_2 and HCHO were measured during the first deployment of the Atmospheric Tomography Mission (ATom-1) aboard the NASA DC-8 aircraft. During the flight on August 1 and 2, 2016, from 14:30 to 00:39 UTC, the aircraft flew from California to the western Arctic, making continuous SO_2 and HCHO measurements, including at <2000 m agl (above ground level) at five locations: Beaufort Sea 1, Beaufort Sea 2, Deadhorse, Fairbanks, and Anchorage (Table S1). SO_2 was measured using the Caltech time-of-flight chemical ionization mass spectrometer (CIT-CIMS),[60] via reaction with the CF_3O^- reagent ion and subsequent monitoring of ions at m/z 83 (FSO_2^-) and m/z 101 ($FSO_2{\cdot}H_2O^-$). The NASA In Situ Airborne Formaldehyde instrument[61] measured formaldehyde using laser-induced fluorescence with a 2σ limit of detection (LOD) of 36 ppt.

Fog droplet HMS production rates were calculated on the basis of estimated liquid water content (LWC) and measured SO_2 and HCHO. SO_2 partitioning to fog results in a pH-dependent equilibrium distribution among SO_2, HSO_3^-, and SO_3^{2-} for subsequent reaction with HCHO (reactions R1 and R2).[9,10,19,20,62]

$$HCHO + HSO_3^- \overset{k_1}{\leftrightarrow} CH_2(OH)SO_3^- \quad (R1)$$

$$HCHO + SO_3^{2-} \overset{k_2}{\leftrightarrow} CH_2(O^-)SO_3^- \quad (R2)$$

HMS production rates (P_{HMS}) are calculated using eq E1:

$$P_{HMS} = (k_1\alpha_1 + k_2\alpha_2)[SO_{2(aq)}][HCHO_{(aq)}] \times LWC \times M_{HMS} \quad (E1)$$

where k_1 (777.8 $mM^{-1}\,h^{-1}$) and k_2 (5.59 × 10^7 $mM^{-1}\,h^{-1}$) are the forward rate constants for R1 and R2, respectively, at the campaign average temperature (276.35 K). α_1 and α_2 are the HSO_3^- and SO_3^{2-} fractions, respectively, based on SO_2 equilibrium and pH. $SO_{2(aq)}$ and $HCHO_{(aq)}$ concentrations were calculated from $SO_{2(g)}$ and $HCHO_{(g)}$, respectively, using their Henry's law constants (0.0288 mol m^{-3} Pa^{-1} for SO_2 and 0.1593 mol m^{-3} Pa^{-1} for HCHO) at the campaign average temperature.[63] Mass transport processes do not limit P_{HMS}, as discussed in the Supporting Information. The fog droplet LWC was estimated from visibility data using the previously reported relationship between LWC and visibility at Utqiaġvik, AK.[53] M_{HMS} is the HMS molecular weight.

RESULTS AND DISCUSSION

Regional Fog across the North Slope of Alaska Oil Fields. Fog was frequently observed at Oliktok Point, AK, from August 18 to September 19, 2016 (Figure S3). Periods of fog were identified by reduced visibility (<10 km), high RH (>80%), minimal precipitation (<0.1 mm h^{-1}), low wind speed (<8 m/s), and local observations, when available. Fog periods lasted for 44 min, on average (ranged from 10 min to 7.5 h), and accounted for 7% of the campaign time; 72% of the fog occurred between 21:00 and 9:00 AKDT when the temperature was lower and the RH was higher. Fog events at Oliktok Point were accompanied by fog at one or more of the three closest airports (Deadhorse, Ugnu-Kuparuk, and Nuiqsut) during 67% of the campaign (Figure S3), even though the airports are located 20−70 km away (Figure S1). At Utqiaġvik, fog events occurred 23% of the time and overlapped with 46% of the fog time at Oliktok Point, despite being located ∼270 km away. This demonstrates that fog often formed on a regional scale, covering the oil fields and surrounding region of the North Slope of Alaska. This is in agreement with previous work showing that fog can be widespread across the Beaufort Sea[57] and is most abundant in the Arctic from June to September.[64]

Individual HMS-Containing Particles. The ATOFMS measured 1100 individual particles containing HMS at Oliktok Point, AK, from August 22 to September 17, 2016.[49] These particles were 3.3% of the total number measured in the size range of 0.07−1.6 μm.[49] During fog periods, the number fraction of HMS-containing particles was 7%, which is comparable to the fraction observed during Beijing winter haze of ∼10%.[32] Eighty-one percent of the HMS-containing particles, by number, were classified as organic carbon particles containing alkylamines and sulfate (OC-amine-sulfate particles).[49] The remaining HMS-containing particles were classified as ECOC (15%, by number), EC (2%), and mineral dust (1%). This is in approximate order of expected particle hygroscopicity, as previously observed by Whiteaker and Prather;[36] the most hygroscopic particles will be more likely to take up water and form fog droplets, promoting HMS formation in the aqueous phase. The observed particle types were previously determined to be most abundant during oil field plumes and emitted locally within the oil fields from industrial and diesel combustion sources.[49] As discussed below, both the OC-amine-sulfate and ECOC particles were internally mixed with oxidized organic carbon and sulfate (see the Supporting Information), consistent with aqueous-phase processing[65] and previous observation of HMS formation within individual internally mixed OC and sulfate particles.[36]

Individual OC-amine-sulfate and ECOC particles comprised 96% of the identified HMS-containing particles. Due to desorption/ionization matrix effects that impact ion signals between particles of significantly different composition,[66] we focus here on these two carbonaceous sulfate particle types. The number percentage of these particles containing HMS was significantly higher ($p = 0.004$, unpaired t-test) when fog was present (average of 12%, range of 0−34%), compared to when fog was not present (average of 5%, range of 0−20%) (Figure 1). HMS was present at higher levels within the individual particles during fog ($p = 0.07$). The average relative peak area, which is proportional to mass, of the ion at m/z −111 was 20% higher during fog for these HMS-containing particles (Figure 1). As in previous studies,[27,29,32,33,36,39−42] the measured particles here correspond to interstitial aerosol, rather than fog droplet residues. The enhancement during fog is consistent with aqueous-phase HMS formation, likely within fog droplets,[9,19−23] followed by droplet evaporation.

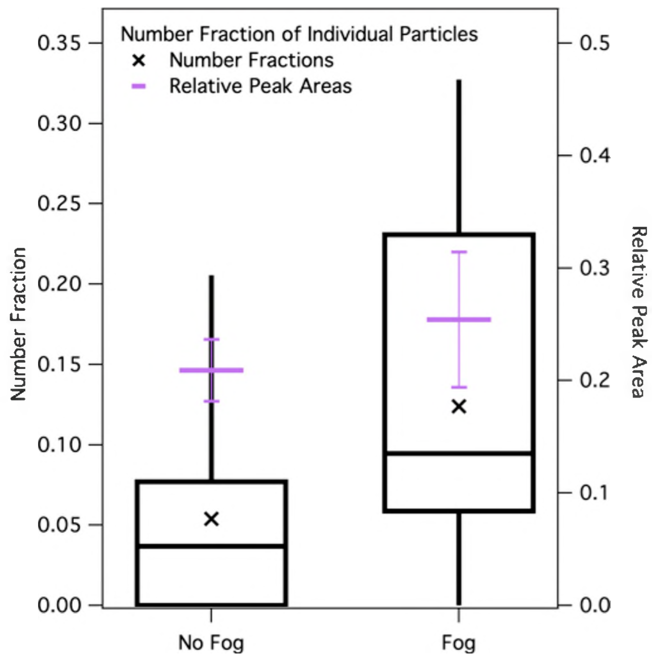

Figure 1. Number fractions of individual OC-amine-sulfate and ECOC particles, measured by the ATOFMS, containing HMS (m/z −111) during fog and no fog periods. The boxes show 25th, 50th, and 75th percentiles; the whiskers show 5th and 95th percentiles, and the markers show mean fractions. The average HMS (m/z −111) relative peak areas, with 95% confidence intervals, for HMS-containing OC-amine-sulfate and ECOC particles are shown during fog and no fog periods. The average number fractions and HMS relative peak areas are significantly higher (p = 0.004 and 0.07, respectively) during fog than during no fog conditions.

The individual HMS-containing OC-amine-sulfate and ECOC particles had additional chemical composition differences when compared to particles that did not contain HMS (Figure 2 and Figure S4). The HMS-containing OC-amine-sulfate and ECOC particles were characterized by larger sulfate

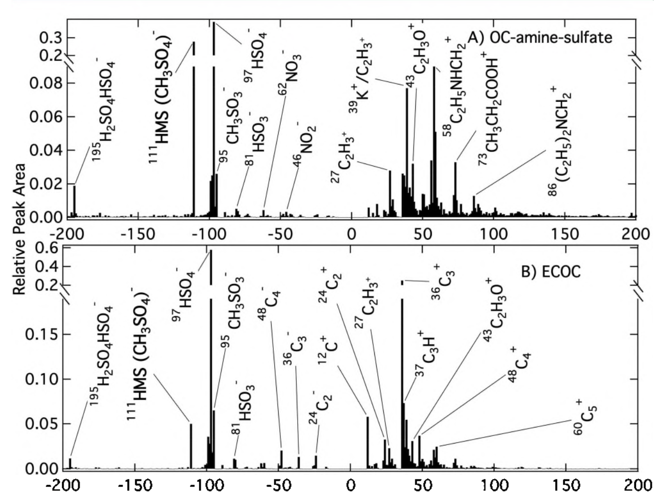

Figure 2. Average individual particle mass spectra for (A) OC-amine-sulfate and (B) ECOC particles that contained HMS (m/z −111).

[m/z −97 (HSO_4^-) and m/z −81 (HSO_3^-)] peak areas, relative to those not containing HMS. Additional sulfate-containing ions, including those at m/z 175 ($K_2HSO_4^+$) and m/z 213 ($K_3SO_4^+$), were at least 4 times more frequently observed in HMS-containing particles. A higher sulfate mass within the individual particles is consistent with aqueous-phase production of both HMS and sulfate,[6,7,9,67] as well as sulfate formation where HMS is an intermediate product.[68,69] Oxidized organic carbon was also more abundant [larger m/z 43 ($C_2H_3O^+$) peak area] for HMS-containing particles and is indicative of a higher organic aerosol oxidation state,[70] consistent with aqueous processing.[71] Sulfuric acid [m/z −195 ($H_2SO_4HSO_4^-$)] and amines {m/z 58 ($C_2H_3NHCH_2^+$), 59 [$N(CH_3)_3^+$], 86 [$(C_2H_5)_2NCH_2^+$], and 118 [$(C_2H_5)_3NOH^+$]} were less abundant, exhibiting smaller peak areas (reduced mass), in the HMS-containing particles. The extent of amine uptake is reduced for less acidic particles,[72,73] consistent with the lower observed sulfuric acid content and higher pH required for HMS formation.[9,19,74]

Bulk PM_1 HMS Mass Concentrations. From August 18 to September 18, 2016, bulk PM_1 HMS mass concentrations for 1−4 day filter samples ranged from below the IC limit of detection (0.3 ng/m^3) to 1.6 ng/m^3 (Figure S5). To the best of our knowledge, these are the first Arctic HMS measurements, which will aid in the evaluation of global models.[34,44] In comparison, the PM_1 sulfate concentration, measured by IC, ranged from 37 to 222 ng/m^3. While these PM_1 sulfate and HMS mass concentrations are low compared to those of midlatitude polluted regions, these levels are important in the rapidly changing Arctic, where sulfate is simulated to have a significant negative radiative forcing impact.[79] When HMS was present, the IC HMS/sulfate molar ratios ranged from 0.01 to 0.02, with these ratios and HMS mass concentrations in line with global modeling of more polluted North American locations during wintertime.[44] Because the level of HMS production is increased at lower temperatures,[44] it is important to note that this late summer Arctic study had an average air temperature of 3.2 °C, more similar to lower latitude wintertime conditions.

Co-located online aerosol chemical speciation monitor [ACSM[75,76] (described in the Supporting Information)] measurements[49] show agreement with the IC sulfate mass concentrations (Figure S6). However, the significantly higher ACSM excess sulfate signal (SO^+ and SO_2^+ signals beyond that attributed to inorganic sulfate),[32] compared to the IC measured HMS concentration (Figure S5), highlights the uncertainty in attributing this ACSM excess sulfate signal solely to HMS, as shown in a recent study.[77] This suggests that additional organosulfur compounds contributed to the ACSM excess sulfate, which ranged from 7 to 33 ng/m^3, on average, during the filter sampling periods. Moffett et al.[78] reported methanesulfonate concentrations ranging from 2 to 41 ng/m^3 at Oliktok Point during the summers of 2015−2017, which included this study. Therefore, this marine organosulfur compound likely explains a significant fraction of the ACSM excess sulfate signal at this coastal site.

Comparison of HMS Production Rates among Alaskan Oil Field, Marine, and Urban Sites. Potential HMS production rates were calculated for Deadhorse [located within the North Slope of Alaska oil fields (Figure S1)] and compared to those of two sites over the upwind Beaufort Sea, as well as the high-latitude cities of Fairbanks and Anchorage, AK (Figure 3). These calculations used the campaign average

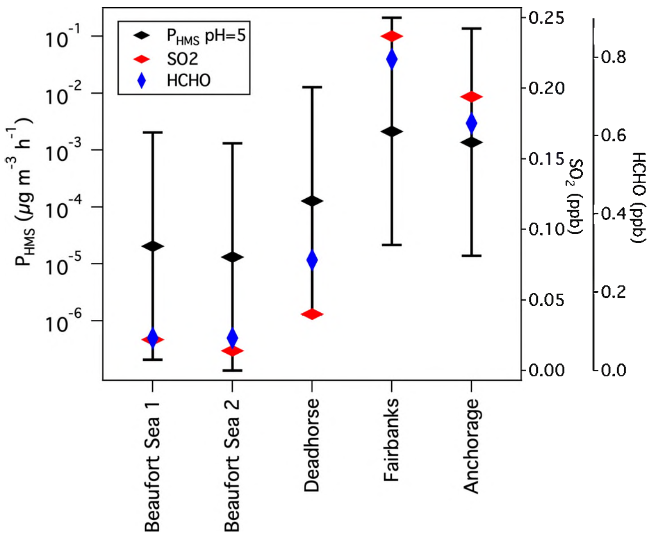

Figure 3. Calculated HMS production rates, shown on a log scale and constrained by measured SO_2 and HCHO mole ratios at these locations, using the campaign average estimated fog LWC (4.8 mg/m^3) and measured temperature (276 K) at Oliktok Point, AK. Boundary layer SO_2 and HCHO mole ratios from the ATom-1 aircraft measurements on August 1 and 2, 2016, for five locations are shown (described in Table S1): Beaufort Sea 1, Beaufort Sea 2, Deadhorse (within the North Slope of Alaska oil fields), Anchorage, and Fairbanks. The SO_2 mole ratios shown and used in the calculations for the two Beaufort Sea sites correspond to 0.5 times the LOD (defined as 3 times the standard deviation of the background measurement, for 1 min averaging, at that location). Bars show the pH range from 4 (bottom bar) to 6 (top bar).

temperature, calculated fog LWC, and near-surface (<2000 m agl) SO_2 and HCHO mole ratios from clear-air aircraft-based measurements during August 1 and 2, 2016 (Table S1). Given the pH sensitivity of HMS production,[9,19,32] the fog pH was assumed to be 5 and varied from 4 to 6, based on typical fogwater pH[80] and previous HMS studies,[9,10,19,32,74,80] which showed HMS decomposition above pH 6 and a reduced level of HMS formation below pH 4.[27,43,74,77,81,82] The HMS production rate within the oil fields was calculated to be 0.12 ng m^{-3} h^{-1}, for SO_2 and HCHO levels of 40 and 282 ppt, respectively (Figure 3). The SO_2/HCHO ratio of 0.14 suggests that HMS production was SO_2 limited within the oil fields.[34] The HMS production rate is highly sensitive to pH and increases 2 orders of magnitude from pH 4 to 6. Other factors, including the LWC uncertainty and lack of ground-based SO_2 and HCHO measurements during fog, contribute to the high HMS production rate uncertainty.

Potential fog HMS production rate estimates for the cities of Fairbanks (average values for SO_2 of 237 ppt and for HCHO of 794 ppt) and Anchorage (average values for SO_2 of 194 ppt and for HCHO of 631 ppt) are 1.4−2.1 ng m^{-3} h^{-1}, an order of magnitude higher than within the oil fields (Figure 3 and Table S1). At these mole ratios, HMS production is predicted to be limited by SO_2.[34] The potential for fog-based HMS production in these high-latitude cities is notable as this chemistry could potentially explain the missing organosulfate source contributing to Fairbanks air quality issues.[83]

The HMS production rate within the North Slope of Alaska oil fields was estimated to be ∼10 times higher than that of the Arctic background (Beaufort Sea 1 and 2, located upwind of the oil fields), where SO_2 levels were below measurement limits of detection and the HCHO level was 83 ppt (Figure 3 and Table S1). This suggests that fog processing within and downwind of the North Slope of Alaska oil fields impacts the atmospheric composition. Fog-based HMS formation likely occurs in other areas of the Arctic influenced by shipping, oil and gas extraction activities, and smelters. This is particularly important to consider because the Arctic is home to major SO_2 sources, including the metal smelters in Norilsk, Russia (one of the largest global SO_2 sources), as well as periodic volcanic eruptions.[84] Rapid warming and declining sea ice in the Arctic[85,86] is making the region more accessible to oil and gas extraction and shipping.[45,46,87] Observational and modeling studies are needed to further evaluate the importance of Arctic aqueous aerosol formation and the HMS contribution to the Arctic atmospheric sulfur budget.

AUTHOR INFORMATION

Corresponding Author

Kerri A. Pratt − *Department of Chemistry and Department of Earth & Environmental Sciences, University of Michigan, Ann Arbor, Michigan 48109, United States*; orcid.org/0000-0003-4707-2290; Email: prattka@umich.edu

Authors

Jun Liu − *Department of Chemistry, University of Michigan, Ann Arbor, Michigan 48109, United States*

Matthew J. Gunsch − *Department of Chemistry, University of Michigan, Ann Arbor, Michigan 48109, United States*

Claire E. Moffett − *Department of Environmental Science, Baylor University, Waco, Texas 76798, United States*

Lu Xu − *Division of Geological and Planetary Sciences, California Institute of Technology, Pasadena, California 91125, United States*; orcid.org/0000-0002-0021-9876

Rime El Asmar − *School of Earth and Atmospheric Sciences, Georgia Institute of Technology, Atlanta, Georgia 30318, United States*

Qi Zhang − *Department of Environmental Toxicology, University of California, Davis, California 95616, United States*; orcid.org/0000-0002-5203-8778

Thomas B. Watson − *Department of Environmental and Climate Sciences, Brookhaven National Laboratory, Upton, New York 11973, United States*

Hannah M. Allen − *Division of Geological and Planetary Sciences, California Institute of Technology, Pasadena, California 91125, United States*

John D. Crounse − *Division of Engineering and Applied Science, California Institute of Technology, Pasadena, California 91125, United States*; orcid.org/0000-0001-5443-729X

Jason St. Clair − *Atmospheric Chemistry and Dynamics Lab, NASA Goddard Space Flight Center, Greenbelt, Maryland 20771, United States; Joint Center for Earth Systems Technology, University of Maryland Baltimore County, Baltimore, Maryland 21228, United States*

Michelle Kim − *Division of Engineering and Applied Science, California Institute of Technology, Pasadena, California 91125, United States*

Paul O. Wennberg − *Division of Geological and Planetary Sciences and Division of Engineering and Applied Science, California Institute of Technology, Pasadena, California 91125, United States*; orcid.org/0000-0002-6126-3854

Rodney J. Weber − *School of Earth and Atmospheric Sciences, Georgia Institute of Technology, Atlanta, Georgia 30318, United States*; orcid.org/0000-0003-0765-8035

Rebecca J. Sheesley − *Department of Environmental Science, Baylor University, Waco, Texas 76798, United States*

ACKNOWLEDGMENTS

This study was supported by the NOAA Climate Program Office and Atmospheric Chemistry, Carbon Cycle, and Climate Program through NA14OAR4310149 (University of Michigan) and NA14OAR4310150 (Baylor University) and a Department of Energy (DOE) Early Career Award (DE-SC0019172). The field work was also supported in part by the DOE Office of Biological and Environmental Research (BER) ARM Climate Research Facility (field campaign 2013-6660). This research was also supported by a National Academies of Sciences, Engineering, and Medicine Gulf Research Program Early-Career Research Fellowship (2000007270). Q.Z. was supported by funding from the DOE Atmospheric System Research Program (DE-SC0017041). R.J.W. and R.E.A. were supported by the NSF Navigating the New Arctic (NNA) program (ICER-1927778). Meteorological and greenhouse gas data were obtained from the ARM Climate Research Facility. DOE ARM, Sandia National Laboratory, AMF3 field operators, and the U.S. Air Force are thanked for logistical assistance at Oliktok Point, AK. Ningxin Wang (University of California, Davis, Davis, CA) is thanked for assistance in analyzing the ACSM data, and Thomas Hanisco (NASA Goddard) and Glenn Wolfe (University of Maryland Baltimore County) are acknowledged for HCHO data contributions. The aircraft data were supported by the NASA ATom Earth Venture Suborbital-2 Program; the authors thank the pilots, technicians, and mechanics for their support during the ATom flights. ATom SO_2 observations were supported by NASA (NNX15AG61A). ATom HCHO observations were supported by the NASA Upper Atmospheric Research Program and the NASA Tropospheric Composition Program. ATOFMS data are available at the DOE ARM data archive (https://www.arm.gov/research/campaigns/amf2015saansa). The authors thank Shaojie Song for helpful discussions of the HMS production calculations.

REFERENCES

(1) Ervens, B.; Turpin, B.; Weber, R. Secondary organic aerosol formation in cloud droplets and aqueous particles (aqSOA): a review

of laboratory, field and model studies. *Atmos. Chem. Phys.* **2011**, *11* (21), 11069−11102.
(2) Herrmann, H.; Schaefer, T.; Tilgner, A.; Styler, S. A.; Weller, C.; Teich, M.; Otto, T. Tropospheric aqueous-phase chemistry: kinetics, mechanisms, and its coupling to a changing gas phase. *Chem. Rev.* **2015**, *115* (10), 4259−4334.
(3) Graedel, T.; Weschler, C. Chemistry within aqueous atmospheric aerosols and raindrops. *Rev. Geophys.* **1981**, *19* (4), 505−539.
(4) Ervens, B. Modeling the processing of aerosol and trace gases in clouds and fogs. *Chem. Rev.* **2015**, *115* (10), 4157−4198.
(5) Blando, J. D.; Turpin, B. J. Secondary organic aerosol formation in cloud and fog droplets: a literature evaluation of plausibility. *Atmos. Environ.* **2000**, *34* (10), 1623−1632.
(6) Hegg, D. A. The importance of liquid-phase oxidation of SO_2 in the troposphere. *J. Geophys. Res.* **1985**, *90* (D2), 3773−3779.
(7) Lelieveld, J.; Heintzenberg, J. Sulfate cooling effect on climate through in-cloud oxidation of anthropogenic SO_2. *Science* **1992**, *258* (5079), 117−120.
(8) Calvert, J. G.; Lazrus, A.; Kok, G. L.; Heikes, B. G.; Walega, J. G.; Lind, J.; Cantrell, C. A. Chemical mechanisms of acid generation in the troposphere. *Nature* **1985**, *317* (6032), 27.
(9) Munger, J. W.; Tiller, C.; Hoffmann, M. R. Identification of hydroxymethanesulfonate in fog water. *Science* **1986**, *231* (4735), 247−249.
(10) Munger, J. W.; Collett, J., Jr; Daube, B., Jr; Hoffmann, M. R. Fogwater chemistry at riverside, California. *Atmos. Environ., Part B* **1990**, *24* (2), 185−205.
(11) Fortems-Cheiney, A.; Chevallier, F.; Pison, I.; Bousquet, P.; Saunois, M.; Szopa, S.; Cressot, C.; Kurosu, T.; Chance, K.; Fried, A. The formaldehyde budget as seen by a global-scale multi-constraint and multi-species inversion system. *Atmos. Chem. Phys.* **2012**, *12* (15), 6699−6721.
(12) Wagner, T.; Wyszyński, M. Aldehydes and ketones in engine exhaust emissions—a review. *Proc. Inst. Mech. Eng., Part D* **1996**, *210* (2), 109−122.
(13) Lee, M.; Heikes, B. G.; Jacob, D. J. Enhancements of hydroperoxides and formaldehyde in biomass burning impacted air and their effect on atmospheric oxidant cycles. *Journal of Geophysical Research: Atmospheres* **1998**, *103* (D11), 13201−13212.
(14) Chin, M.; Jacob, D. J. Anthropogenic and natural contributions to tropospheric sulfate: A global model analysis. *Journal of Geophysical Research: Atmospheres* **1996**, *101* (D13), 18691−18699.
(15) Spiro, P. A.; Jacob, D. J.; Logan, J. A. Global inventory of sulfur emissions with 1× 1 resolution. *J. Geophys. Res.* **1992**, *97* (D5), 6023−6036.
(16) Chin, M.; Jacob, D. J.; Gardner, G. M.; Foreman-Fowler, M. S.; Spiro, P. A.; Savoie, D. L. A global three-dimensional model of tropospheric sulfate. *Journal of Geophysical Research: Atmospheres* **1996**, *101* (D13), 18667−18690.
(17) Yang, Y.; Wang, H.; Smith, S. J.; Easter, R. C.; Rasch, P. J. Sulfate aerosol in the Arctic: Source attribution and radiative forcing. *J. Geophys. Res.: Atmos.* **2018**, *123* (3), 1899−1918.
(18) Chen, K.; Zhao, J. Theoretical investigation of a potentially important formation pathway of organosulfate in atmospheric aqueous aerosols. *Sci. Rep.* **2020**, *10* (1), 6299.
(19) Munger, J.; Jacob, D.; Hoffmann, M. The occurrence of bisulfite-aldehyde addition products in fog-and cloudwater. *J. Atmos. Chem.* **1984**, *1* (4), 335−350.
(20) Munger, J. W.; Jacob, D. J.; Waldman, J. M.; Hoffmann, M. R. Fogwater chemistry in an urban atmosphere. *Journal of Geophysical Research: Oceans* **1983**, *88* (C9), 5109−5121.
(21) Rao, X.; Collett, J. L. J. Behavior of S (IV) and formaldehyde in a chemically heterogeneous cloud. *Environ. Sci. Technol.* **1995**, *29* (4), 1023−1031.
(22) Facchini, M.; Fuzzi, S.; Lind, J.; Fierlinger-Oberlinninger, H.; Kalina, M.; Puxbaum, H.; Winiwarter, W.; Arends, B.; Wobrock, W.; Jaeschke, W.; et al. Phase-partitioning and chemical reactions of low molecular weight organic compounds in fog. *Tellus, Ser. B* **1992**, *44* (5), 533−544.
(23) Joos, F.; Baltensperger, U. A field study on chemistry, S (IV) oxidation rates and vertical transport during fog conditions. *Atmos. Environ., Part A* **1991**, *25* (2), 217−230.
(24) Ang, C. C.; Lipari, F.; Swarin, S. J. Determination of hydroxymethanesulfonate in wet deposition samples. *Environ. Sci. Technol.* **1987**, *21* (1), 102−105.
(25) Zuo, Y.; Chen, H. Simultaneous determination of sulfite, sulfate, and hydroxymethanesulfonate in atmospheric waters by ion-pair HPLC technique. *Talanta* **2003**, *59* (5), 875−881.
(26) Chapman, E.; Barinaga, C.; Udseth, H.; Smith, R. Confirmation and quantitation of hydroxymethanesulfonate in precipitation by electrospray ionization-tandem mass spectrometry. *Atmos. Environ., Part A* **1990**, *24* (12), 2951−2957.
(27) Dixon, R. W.; Aasen, H. Measurement of hydroxymethanesulfonate in atmospheric aerosols. *Atmos. Environ.* **1999**, *33* (13), 2023−2029.
(28) Murphy, D.; Thomson, D.; Mahoney, M. In situ measurements of organics, meteoritic material, mercury, and other elements in aerosols at 5 to 19 kilometers. *Science* **1998**, *282* (5394), 1664−1669.
(29) Scheinhardt, S.; Van Pinxteren, D.; Müller, K.; Spindler, G.; Herrmann, H. Hydroxymethanesulfonic acid in size-segregated aerosol particles at nine sites in Germany. *Atmos. Chem. Phys.* **2014**, *14* (9), 4531−4538.
(30) Dabek-Zlotorzynska, E.; Aranda-Rodriguez, R.; Graham, L. Capillary electrophoresis determinative and GC-MS confirmatory method for water-soluble organic acids in airborne particulate matter and vehicle emission. *J. Sep. Sci.* **2005**, *28* (13), 1520−1528.
(31) Dabek-Zlotorzynska, E.; Piechowski, M.; Keppel-Jones, K.; Aranda-Rodriguez, R. Determination of hydroxymethanesulfonic acid in environmental samples by capillary electrophoresis. *J. Sep. Sci.* **2002**, *25* (15−17), 1123−1128.
(32) Song, S.; Gao, M.; Xu, W.; Sun, Y.; Worsnop, D. R.; Jayne, J. T.; Zhang, Y.; Zhu, L.; Li, M.; Zhou, Z.; et al. Possible heterogeneous chemistry of hydroxymethanesulfonate (HMS) in northern China winter haze. *Atmos. Chem. Phys.* **2019**, *19* (2), 1357−1371.
(33) Ma, T.; Furutani, H.; Duan, F.; Kimoto, T.; Jiang, J.; Zhang, Q.; Xu, X.; Wang, Y.; Gao, J.; Geng, G.; et al. Contribution of hydroxymethanesulfonate (HMS) to severe winter haze in the North China Plain. *Atmos. Chem. Phys.* **2020**, *20* (10), 5887−5897.
(34) Moch, J. M.; Dovrou, E.; Mickley, L. J.; Keutsch, F. N.; Liu, Z.; Wang, Y.; Dombek, T. L.; Kuwata, M.; Budisulistiorini, S. H.; Yang, L.; et al. Global importance of hydroxymethanesulfonate in ambient particulate matter: Implications for air quality. *J. Geophys. Res.: Atmos.* **2020**, *125* (18), e2020JD032706.
(35) Wei, L.; Fu, P.; Chen, X.; An, N.; Yue, S.; Ren, H.; Zhao, W.; Xie, Q.; Sun, Y.; Zhu, Q.-F.; et al. Quantitative Determination of Hydroxymethanesulfonate (HMS) Using Ion Chromatography and UHPLC-LTQ-Orbitrap Mass Spectrometry: A Missing Source of Sulfur during Haze Episodes in Beijing. *Environ. Sci. Technol. Lett.* **2020**, *7* (10), 701−707.
(36) Whiteaker, J. R.; Prather, K. A. Hydroxymethanesulfonate as a tracer for fog processing of individual aerosol particles. *Atmos. Environ.* **2003**, *37* (8), 1033−1043.
(37) Neubauer, K. R.; Johnston, M. V.; Wexler, A. S. On-line analysis of aqueous aerosols by laser desorption ionization. *Int. J. Mass Spectrom. Ion Processes* **1997**, *163* (1−2), 29−37.
(38) Neubauer, K. R.; Sum, S. T.; Johnston, M. V.; Wexler, A. S. Sulfur speciation in individual aerosol particles. *Journal of Geophysical Research: Atmospheres* **1996**, *101* (D13), 18701−18707.
(39) Dall'Osto, M.; Harrison, R.; Coe, H.; Williams, P. Real-time secondary aerosol formation during a fog event in London. *Atmos. Chem. Phys.* **2009**, *9* (7), 2459−2469.
(40) Zhang, G.; Bi, X.; Chan, L. Y.; Li, L.; Wang, X.; Feng, J.; Sheng, G.; Fu, J.; Li, M.; Zhou, Z. Enhanced trimethylamine-containing particles during fog events detected by single particle aerosol mass spectrometry in urban Guangzhou, China. *Atmos. Environ.* **2012**, *55*, 121−126.

(41) Lee, S. H.; Murphy, D. M.; Thomson, D. S.; Middlebrook, A. M. Nitrate and oxidized organic ions in single particle mass spectra during the 1999 Atlanta Supersite Project. *J. Geophys. Res.* **2003**, *108* (D7), SOS 5-1−SOS 5-8.
(42) Lee, S. H.; Murphy, D. M.; Thomson, D. S.; Middlebrook, A. M. Chemical components of single particles measured with Particle Analysis by Laser Mass Spectrometry (PALMS) during the Atlanta SuperSite Project: Focus on organic/sulfate, lead, soot, and mineral particles. *J. Geophys. Res.* **2002**, *107* (D1), AAC 1-1−AAC 1-13.
(43) Moch, J. M.; Dovrou, E.; Mickley, L. J.; Keutsch, F. N.; Cheng, Y.; Jacob, D. J.; Jiang, J.; Li, M.; Munger, J. W.; Qiao, X.; et al. Contribution of hydroxymethane sulfonate to ambient particulate matter: A potential explanation for high particulate sulfur during severe winter haze in Beijing. *Geophys. Res. Lett.* **2018**, *45* (21), 11969−11979.
(44) Song, S.; Ma, T.; Zhang, Y.; Shen, L.; Liu, P.; Li, K.; Zhai, S.; Zheng, H.; Gao, M.; Moch, J. M.; Duan, F.; He, K.; McElroy, M. B. Global modeling of heterogeneous hydroxymethanesulfonate chemistry. *Atmos. Chem. Phys.* **2021**, *21* (1), 457−481.
(45) Schmale, J.; Arnold, S.; Law, K. S.; Thorp, T.; Anenberg, S.; Simpson, W.; Mao, J.; Pratt, K. Local Arctic air pollution: A neglected but serious problem. *Earth's Future* **2018**, *6* (10), 1385−1412.
(46) Peters, G.; Nilssen, T.; Lindholt, L.; Eide, M.; Glomsrød, S.; Eide, L.; Fuglestvedt, J. Future emissions from shipping and petroleum activities in the Arctic. *Atmos. Chem. Phys.* **2011**, *11* (11), 5305−5320.
(47) Roiger, A.; Thomas, J.-L.; Schlager, H.; Law, K. S.; Kim, J.; Schäfler, A.; Weinzierl, B.; Dahlkötter, F.; Krisch, I.; Marelle, L.; et al. Quantifying emerging local anthropogenic emissions in the Arctic region: The ACCESS aircraft campaign experiment. *Bull. Am. Meteorol. Soc.* **2015**, *96* (3), 441−460.
(48) Jaffe, D.; Honrath, R.; Furness, D.; Conway, T.; Dlugokencky, E.; Steele, L. A determination of the CH_4, NO_x and CO_2 emissions from the Prudhoe Bay, Alaska oil development. *J. Atmos. Chem.* **1995**, *20* (3), 213−227.
(49) Gunsch, M. J.; Liu, J.; Moffett, C. E.; Sheesley, R. J.; Wang, N.; Zhang, Q.; Watson, T. B.; Pratt, K. A. Diesel Soot and Amine-Containing Organic Sulfate Aerosols in an Arctic Oil Field. *Environ. Sci. Technol.* **2019**, *54* (1), 92−101.
(50) Brooks, S. B.; Crawford, T. L.; Oechel, W. C. Measurement of carbon dioxide emissions plumes from Prudhoe Bay, Alaska oil fields. *J. Atmos. Chem.* **1997**, *27* (2), 197−207.
(51) Brock, C. A.; Cozic, J.; Bahreini, R.; Froyd, K. D.; Middlebrook, A. M.; McComiskey, A.; Brioude, J.; Cooper, O.; Stohl, A.; Aikin, K.; et al. Characteristics, sources, and transport of aerosols measured in spring 2008 during the aerosol, radiation, and cloud processes affecting Arctic Climate (ARCPAC) Project. *Atmos. Chem. Phys.* **2011**, *11* (6), 2423−2453.
(52) Gunsch, M. J.; Kirpes, R. M.; Kolesar, K. R.; Barrett, T. E.; China, S.; Sheesley, R. J.; Laskin, A.; Wiedensohler, A.; Tuch, T.; Pratt, K. A. Contributions of transported Prudhoe Bay oil field emissions to the aerosol population in Utqiagvik, Alaska. *Atmos. Chem. Phys.* **2017**, *17*, 10879−10892.
(53) Kumai, M. Arctic fog droplet size distribution and its effect on light attenuation. *J. Atmos. Sci.* **1973**, *30* (4), 635−643.
(54) Nilsson, E. D.; Bigg, E. K. Influences on formation and dissipation of high Arctic fogs during summer and autumn and their interaction with aerosol. *Tellus, Ser. B* **1996**, *48* (2), 234−253.
(55) Bergin, M.; Pandis, S.; Davidson, C.; Jaffrezo, J. L.; Dibb, J. E.; Russell, A.; Kuhns, H. Modeling of the processing and removal of trace gas and aerosol species by Arctic radiation fogs and comparison with measurements. *Journal of Geophysical Research: Atmospheres* **1996**, *101* (D9), 14465−14478.
(56) Zhang, T.; Osterkamp, T.; Stamnes, K. Some characteristics of the climate in northern Alaska, USA. *Arct. Alp. Res.* **1996**, *28* (4), 509−518.
(57) Yi, L.; Li, K.-F.; Chen, X.; Tung, K.-K. Arctic fog detection using infrared spectral measurements. *Journal of Atmospheric and Oceanic Technology* **2019**, *36* (8), 1643−1656.
(58) Pratt, K. A.; Mayer, J. E.; Holecek, J. C.; Moffet, R. C.; Sanchez, R. O.; Rebotier, T. P.; Furutani, H.; Gonin, M.; Fuhrer, K.; Su, Y.; et al. Development and characterization of an aircraft aerosol time-of-flight mass spectrometer. *Anal. Chem.* **2009**, *81* (5), 1792−1800.
(59) Song, X.-H.; Hopke, P. K.; Fergenson, D. P.; Prather, K. A. Classification of single particles analyzed by ATOFMS using an artificial neural network, ART-2A. *Anal. Chem.* **1999**, *71* (4), 860−865.
(60) Crounse, J. D.; McKinney, K. A.; Kwan, A. J.; Wennberg, P. O. Measurement of gas-phase hydroperoxides by chemical ionization mass spectrometry. *Anal. Chem.* **2006**, *78* (19), 6726−6732.
(61) Cazorla, M.; Wolfe, G. M.; Bailey, S. A.; Swanson, A. K.; Arkinson, H. L.; Hanisco, T. F. A new airborne laser-induced fluorescence instrument for in situ detection of formaldehyde throughout the troposphere and lower stratosphere. *Atmos. Meas. Tech.* **2015**, *8* (2), 541−552.
(62) Boyce, S. D.; Hoffmann, M. R. Kinetics and mechanism of the formation of hydroxymethanesulfonic acid at low pH. *J. Phys. Chem.* **1984**, *88* (20), 4740−4746.
(63) Sander, R. Compilation of Henry's law constants (version 4.0) for water as solvent. *Atmos. Chem. Phys.* **2015**, *15* (8), 4399−4981.
(64) Eastman, R.; Warren, S. G. Interannual variations of Arctic cloud types in relation to sea ice. *J. Clim.* **2010**, *23* (15), 4216−4232.
(65) Ge, X.; Zhang, Q.; Sun, Y.; Ruehl, C. R.; Setyan, A. Effect of aqueous-phase processing on aerosol chemistry and size distributions in Fresno, California, during wintertime. *Environmental Chemistry* **2012**, *9* (3), 221−235.
(66) Hatch, L. E.; Pratt, K. A.; Huffman, J. A.; Jimenez, J. L.; Prather, K. A. Impacts of aerosol aging on laser desorption/ionization in single-particle mass spectrometers. *Aerosol Sci. Technol.* **2014**, *48* (10), 1050−1058.
(67) Hoag, K. J.; Collett, J. L., Jr; Pandis, S. N. The influence of drop size-dependent fog chemistry on aerosol processing by San Joaquin Valley fogs. *Atmos. Environ.* **1999**, *33* (29), 4817−4832.
(68) Barlow, S.; Buxton, G. V.; Murray, S. A.; Salmon, G. A. Free-radical-induced oxidation of hydroxymethanesulfonate in aqueous solution Part 1A pulse radiolysis study of the reactions of OHand SO 4. *J. Chem. Soc., Faraday Trans.* **1997**, *93* (20), 3637−3640.
(69) Barlow, S.; Buxton, G. V.; Murray, S. A.; Salmon, G. A. Free-radical-induced oxidation of hydroxymethanesulfonate in aqueous solution Part 2A pulse and steady-state radiolysis study of oxygenated solutions. *J. Chem. Soc., Faraday Trans.* **1997**, *93* (20), 3641−3645.
(70) Qin, X.; Pratt, K. A.; Shields, L. G.; Toner, S. M.; Prather, K. A. Seasonal comparisons of single-particle chemical mixing state in Riverside, CA. *Atmos. Environ.* **2012**, *59*, 587−596.
(71) McNeill, V. F. Aqueous Organic Chemistry in the Atmosphere: Sources and Chemical Processing of Organic Aerosols. *Environ. Sci. Technol.* **2015**, *49* (3), 1237−1244.
(72) Rehbein, P. J.; Jeong, C.-H.; McGuire, M. L.; Yao, X.; Corbin, J. C.; Evans, G. J. Cloud and fog processing enhanced gas-to-particle partitioning of trimethylamine. *Environ. Sci. Technol.* **2011**, *45* (10), 4346−4352.
(73) VandenBoer, T.; Petroff, A.; Markovic, M.; Murphy, J. Size distribution of alkyl amines in continental particulate matter and their online detection in the gas and particle phase. *Atmos. Chem. Phys.* **2011**, *11* (9), 4319−4332.
(74) Olson, T.; Hoffmann, M. On the kinetics of formaldehyde-S (IV) adduct formation in slightly acidic solution. *Atmos. Environ. (1967-1989)* **1986**, *20* (11), 2277−2278.
(75) Fröhlich, R.; Cubison, M.; Slowik, J.; Bukowiecki, N.; Prévôt, A.; Baltensperger, U.; Schneider, J.; Kimmel, J.; Gonin, M.; Rohner, U.; et al. The ToF-ACSM: a portable aerosol chemical speciation monitor with TOFMS detection. *Atmos. Meas. Tech.* **2013**, *6* (11), 3225−3241.
(76) Ng, N. L.; Herndon, S. C.; Trimborn, A.; Canagaratna, M. R.; Croteau, P. L.; Onasch, T. B.; Sueper, D.; Worsnop, D. R.; Zhang, Q.; Sun, Y. L.; Jayne, J. T. An Aerosol Chemical Speciation Monitor (ACSM) for Routine Monitoring of the Composition and Mass

Concentrations of Ambient Aerosol. *Aerosol Sci. Technol.* **2011**, *45* (7), 780–794.

(77) Dovrou, E.; Lim, C. Y.; Canagaratna, M. R.; Kroll, J. H.; Worsnop, D. R.; Keutsch, F. N. Measurement techniques for identifying and quantifying hydroxymethanesulfonate (HMS) in an aqueous matrix and particulate matter using aerosol mass spectrometry and ion chromatography. *Atmos. Meas. Tech.* **2019**, *12* (10), 5303–5315.

(78) Moffett, C. E.; Barrett, T. E.; Liu, J.; Gunsch, M. J.; Upchurch, L. M.; Quinn, P. K.; Pratt, K. A.; Sheesley, R. J. Long-Term Trends for Marine Sulfur Aerosol in the Alaskan Arctic and Relationships With Temperature. *J. Geophys. Res.: Atmos.* **2020**, *125* (22), e2020JD033225.

(79) Breider, T. J.; Mickley, L. J.; Jacob, D. J.; Ge, C.; Wang, J.; Payer Sulprizio, M.; Croft, B.; Ridley, D. A.; McConnell, J. R.; Sharma, S.; Husain, L.; Dutkiewicz, V. A.; Eleftheriadis, K.; Skov, H.; Hopke, P. K. Multidecadal trends in aerosol radiative forcing over the Arctic: Contribution of changes in anthropogenic aerosol to Arctic warming since 1980. *J. Geophys. Res.: Atmos.* **2017**, *122* (6), 3573–3594.

(80) Pye, H. O.; Nenes, A.; Alexander, B.; Ault, A. P.; Barth, M. C.; Clegg, S. L.; Collett, J. L., Jr; Fahey, K. M.; Hennigan, C. J.; Herrmann, H.; et al. The acidity of atmospheric particles and clouds. *Atmos. Chem. Phys.* **2020**, *20*, 4809–4888.

(81) Olson, T. M.; Hoffmann, M. R. Hydroxyalkylsulfonate formation: its role as a S (IV) reservoir in atmospheric water droplets. *Atmos. Environ. (1967-1989)* **1989**, *23* (5), 985–997.

(82) Betterton, E. A.; Erel, Y.; Hoffmann, M. R. Aldehyde-bisulfite adducts: prediction of some of their thermodynamic and kinetic properties. *Environ. Sci. Technol.* **1988**, *22* (1), 92–99.

(83) Shakya, K. M.; Peltier, R. E. Investigating missing sources of sulfur at Fairbanks, Alaska. *Environ. Sci. Technol.* **2013**, *47* (16), 9332–9338.

(84) Fioletov, V. E.; McLinden, C. A.; Krotkov, N.; Li, C.; Joiner, J.; Theys, N.; Carn, S.; Moran, M. D. A global catalogue of large SO_2 sources and emissions derived from the Ozone Monitoring Instrument. *Atmos. Chem. Phys.* **2016**, *16* (18), 11497–11519.

(85) Screen, J. A.; Simmonds, I. The central role of diminishing sea ice in recent Arctic temperature amplification. *Nature* **2010**, *464* (7293), 1334.

(86) Swart, N. C.; Fyfe, J. C.; Hawkins, E.; Kay, J. E.; Jahn, A. Influence of internal variability on Arctic sea-ice trends. *Nat. Clim. Change* **2015**, *5* (2), 86.

(87) Harsem, Ø.; Heen, K.; Rodrigues, J.; Vassdal, T. Oil exploration and sea ice projections in the Arctic. *Polar Rec.* **2015**, *51* (1), 91–106.